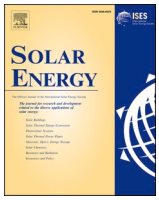
Solar Energy 318 (2026) 115095



Contents lists available at ScienceDirect

Solar Energy

journal homepage: www.elsevier.com/locate/solener





Experimental qualification of a novel fixed-focus parabolic trough collector designed for molten salt

Sonja Kallio [e,*], Martin Eickhoff [a], Daniel Morales [b], Timo Zippler [c], Kenneth Thiede [c], Joachim Krüger [c], Niels Algner [a], Michael Nieslony [a], Eduardo Saez Martinez [a], Benedikt Kölsch [d], Dirk Krüger [d]

[a] DLR (German Aerospace Center) Institute of Solar Research, Almería, 04005, Spain
[b] Ferrum Tecnoindustrial S.L, Spain
[c] Solarlite Beteiligung UG, Germany
[d] DLR (German Aerospace Center) Institute of Solar Research, Cologne, 51147, Germany
[e] DLR (German Aerospace Center) Institute of Future Fuels, Cologne, 51147, Germany

ARTICLE INFO

Keywords:
Parabolic trough
Molten salt
Fixed-focus collector
Qualification
Innovative collector design

ABSTRACT

A parabolic trough collector (PTC) consists of parabolic mirrors that concentrate direct solar radiation onto an absorber tube, in which a heat transfer medium is heated. A typical PTC is a single-axis moving optical system on its concentrator support structure carrying both the parabolic reflectors and the absorber supports. This whole structure is rotated and connected via several pylons. This causes interruptions in the collector row of the plant which is sensitive to failures. Rotation movement and thermal expansion of the receiver tube are absorbed by flexible pipe connectors. These connectors enable the connection between the receiver tube and the fixed pipeline, and are sensitive for frequently reported failures. In this article, an innovative PTC design is presented with the fixed focus principle to eliminate flexible pipe connectors and allow a continuous row of the collectors. The study includes the construction and qualification of a prototype of such a fixed focus PTC, the so-called MS-Trough collector. The mechanical qualification show high rigidity of the collector compared to the state-of-art PTCs. A collector optical efficiency of 74 % and average intercept factor of as high as 86 % are reached. The maximum intercept factor of 94 % is reached on a single collector module. The first erection of the prototype collector gives valuable experience of the MS-Trough collector construction.

1. Introduction

Concentrating solar power (CSP) systems can employ different heat transfer fluids (HTF), such as thermal oil, molten salt, particles, water/steam or air. Depending on the concentration principle, CSP technologies are commonly classified into point focus systems (solar power tower and parabolic dish) and line focus systems (parabolic trough and linear Fresnel collectors) [1]. Among these, parabolic trough collectors (PTCs) represent the most established and commercially deployed CSP technology. Conventional commercial PTC plants typically use synthetic thermal oils as HTF, which limits the operating temperature to approximately 400 °C. Higher operating temperatures can be achieved by alternative HTFs, such as molten salts, but these approaches introduce additional design and operational requirements [2].

By the end of 2024, the global renewable energy capacity reached 4448 GW, of which solar capacity accounted for 1865 GW [3]. However, the globally installed CSP capacity remains only 7.2 GW, installed mainly in Spain, the United States and China [4]. Within the CSP branch, PTCs account for about 66 % of the installed capacity, followed by solar tower (24 %), linear Fresnel (9 %) and dish systems (1 %) [5]. This reflects high technological maturity and cost-effectiveness of PTCs [6].

A conventional PTC consists of a rotating support structure carrying parabolic reflector panels and a linear absorber tube [7]. The reflected solar radiation is concentrated onto a spectrally selective coated, vacuum-insulated receiver (or absorber) tube with a standard diameter of 70, 80, or 90 mm. In commercial solar fields, individual Solar Collector Elements (SCEs) (or collector modules) are connected to form Solar Collector Assemblies (SCAs), which are driven by a common tracking system [5]. While this configuration has proven technically reliable, the combined rotation of both concentrator and receiver tube

* Corresponding author.
E-mail address: sonja.kallio@dlr.de (S. Kallio).

https://doi.org/10.1016/j.solener.2026.115095
Received 11 May 2026; Received in revised form 24 July 2026; Accepted 6 September 2026
Available online 12 September 2026
0038-092X/© 2026 The Authors. Published by Elsevier Ltd on behalf of International Solar Energy Society. This is an open access article under the CC BY license (http://creativecommons.org/licenses/by/4.0/).

introduces structural and operational challenges. In particular, rotation and expansion performing assemblies (REPAs), such as ball joints or flexible hoses, are required at the collector ends to connect the moving receiver tube to the fixed piping system and to compensate for both tracking movement and thermal expansion. These components are exposed to cyclic mechanical loading, elevated temperatures and pressure variations. Previous investigations have shown that temperature, pressure and adjacent piping configuration can significantly influence the mechanical loads acting on flexible pipe connector assemblies [8,9]. Furthermore, friction in bearings and flexible connectors can contribute to torsional deformation of the collector structure, potentially affecting optical alignment and the intercept factor [10].

These challenges become more critical when molten salt is used as HTF. Molten salts enable higher operating temperatures and can improve the thermodynamic efficiency of the power cycle, but they require strict control of thermal expansion, reliable drainage strategies and freeze protection. Previous experimental work has demonstrated the technical feasibility of molten-salt operation in parabolic trough solar fields. The Archimede molten-salt parabolic trough demonstration plant in Massa Martana, Italy, has provided operational experience with solar salt in a stand-alone MSPT configuration [11]. In addition, the MATS project demonstrated a stand-alone and fully integrated 1 MW_e CSP plant using molten salt as HTF in linear parabolic trough collectors in Borg El Arab, Egypt. The MATS solar field comprised about 10,000 m^2 of mirror surface and was operated for more than 2500 h with solar salt circulation under different conditions, including start-up, draining, night circulation and solar tracking tests [12].

In modern commercial PTC systems, continuous efforts have been made at solar-field, component and concept levels to reduce costs and enhance the performance. At the component level, conventional reflector designs typically employ 4–5 mm thick silvered glass mirrors. Thin glass reflectors have been proposed to lower costs and improve optical quality [5]. Krüger et al. [13] demonstrated aluminum-based mirror concepts with improved reflectance and compared them to thick glass. The reflectance was increased from 82.6 % to 92.3 % but did not reach the thin-glass reflectance of 96.5 %. Secondary reflectors have been investigated to homogenize flux distribution and reduce peak thermal stresses on the receiver tube. Depending on the selected secondary-reflector geometry, these approaches can substantially improve flux uniformity while maintaining high optical efficiency. [14] Secondary flat reflectors have also been investigated to increase the concentration ratio and reduce sensitivity to misalignment. However, they may introduce shading and reflection losses and can reduce the overall optical efficiency depending on the geometry and integration concept [15].

On the receiver side, significant research has focused on improving the thermo-hydraulic performance of absorber tubes. Passive enhancement methods using different inserts such as turbulators, fins or twisted tapes have been reviewed in [16]. Although such measures substantially increase heat transfer coefficients, they generally introduce higher pressure losses and increased manufacturing costs of the tube. Bellos et al. [17] reported thermal efficiency improvements of up to 65.6 % using cylindrical inserts, while longitudinal fins have been investigated regarding optimal placement and height [18]. Alternative receiver geometries, including double evacuated tubes [19] and variable-diameter absorber concepts [20], have been proposed to increase operating temperature and efficiency and to reduce costs.

To increase operating temperature range of the PTC and maximize the power cycle efficiency, different HTFs have been investigated. Conventional PTC plants predominantly use synthetic thermal oils with a maximum operating temperature around 400 °C and a freezing temperature of 12 °C [5]. Hilgert et al. [21] successfully demonstrated higher temperatures with a novel silicone-based HTF (HELISOL® 5A) in a PTC environment, reaching an average operating temperature of 425 °C during 480 operating hours. In addition, 450 °C was maintained for 50 h to test the robustness of HELISOL® 5A.

Molten salts represent a promising option for achieving temperatures up to 550 °C, thereby increasing the thermal efficiency of PTC systems. However, their corrosive characteristics and high freezing temperature of about 227 °C impose stringent requirements on system design and continuous freeze protection to avoid damage of the components due to solidification of the salt [5]. Together with Archimede and MATS experience described above, these constraints motivate collector concepts that reduce critical moving HTF connections and simplify the integration of continuous receiver rows [12,22].

Current state-of-the-art PTC concepts, such as EuroTrough [23,24] and HelioTrough® [25], are based on rotating receiver designs with central torque units, on-site assembly jigs and flexible pipe connectors at the collector ends [5]. Several innovative PTC concepts have been presented in the literature with the aim of increasing operating temperature, reducing solar field costs, or improving water consumption [26]. The SkyTrough collector demonstrated lightweight structures and polymer-based reflector films, reducing material costs compared to the EuroTrough state-of-the-art collector by 36 % [27,28]. The use of non-metallic materials, such as high-performance concrete, was demonstrated in the ConSol collector [13]. Enclosed aperture collectors, including the GlassPoint [29] and HelioTube [30] concepts, use transparent covers, such as glass or polymeric membranes, above the collector aperture area to mitigate wind loads and soiling effects. Only a few companies have successfully built and demonstrated fixed-focus PTC pilot plants for direct steam generation up to 500 °C [5,31,32].

To address some of these limitations of conventional rotating-receiver PTC designs, an innovative fixed-focus PTC concept, called MS (Molten Salt)-Trough, was developed at the German Aerospace Center (DLR) in co-operation with Solarlite Beteiligung UG and Ferrum Tecnoindustrial S.L. In this design, the receiver tube remains stationary while only the concentrator structure rotates. The mechanical separation between fixed receiver and rotating reflector structure eliminates the need for flexible pipe connectors at the collector ends and enables a continuous receiver tube along the collector row. The concept further incorporates a lightweight dual torque-box structure aimed at reducing torsional deformation and improving structural rigidity. Fixed-focus or fixed-receiver PTC concepts have been described in previous collector concept reviews, and selected concepts have been reported at prototype or pilot scale [5,29]. However, publicly available peer-reviewed qualification data on full-scale mechanical rigidity, torsional deformation, and optical performance remain limited.

This article presents the first comprehensive qualification of the full-scale MS-Trough prototype. The prototype was erected and experimentally validated in Tabernas, Spain during the period from 03.2024 to 06.2024. The qualification includes mechanical measurements of deflection and torsion, indirect determination of collector optical efficiency through thermal measurements, and drone-based deflectometric assessments of reflector shape accuracy and intercept factor. The results are discussed in comparison with reported performance indicators of state-of-the-art commercial PTC systems and provide an experimental basis for further development of loop-scale molten salt applications. Specifically, this study tests the hypothesis that mechanically decoupling the stationary receiver from the rotating concentrator, together with the dual torque-box structure, can provide full-scale mechanical rigidity and optical performance comparable to established commercial PTCs while eliminating the moving HTF connections that complicate molten-salt operation.

2. Collector design and qualification methods

2.1. Conceptual design

The MS-Trough collector has a light-weight torque frame structure presented in Fig. 1. Instead of a single central torque tube, two decentralized torque boxes are located on both sides of the collector. Two torque boxes and two front beams form a counterweight for the lower concentrator area to avoid collector imbalance and torsional forces, and

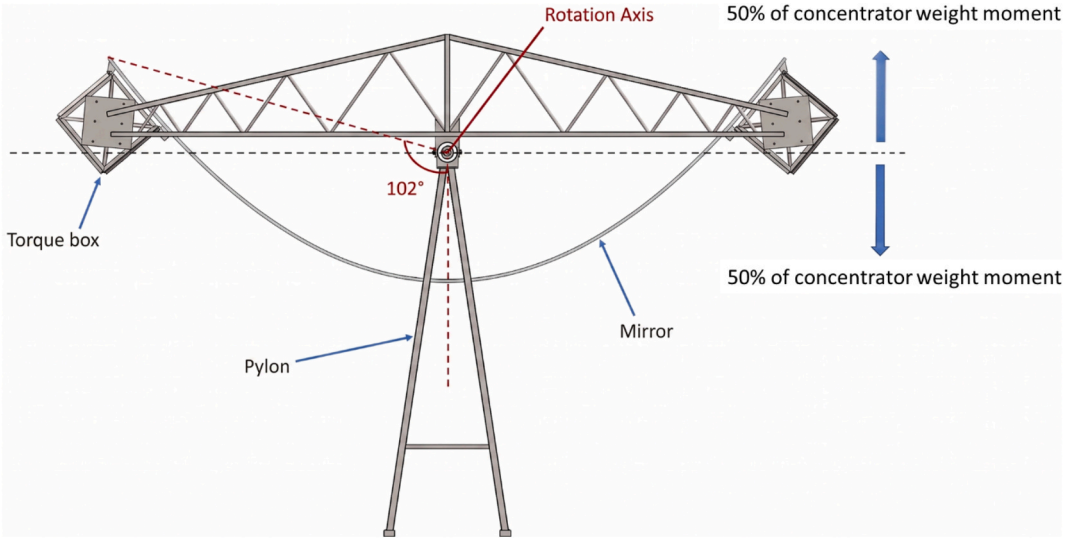


Fig. 1. Steel structure of MS-Trough collector design.

to increase the rigidity of the collector. Additionally, the innovative torsion compensators at the collector ends are used to minimize the torsional deformation, or twisting. As shown in Fig. 1, 50% of the concentrator weight moment is above the rotation axis and other 50 % is below. The reinforcement supports connect the torque boxes and reflectors to maximize the rigidity. The collector design allows the concentrator center of gravity to be in the rotation axis which equals to the receiver tube as shown in Fig. 1.

The MS-Trough collector design is based on fixed-focus which makes it different from the conventional collector designs. The complete separation between the fixed receiver tube and concentrator allows a continuous PTC row up to 1 km and to eliminate the failure-prone flexible pipe connectors. A special sliding rail system is used to allow the absorber tube to slide freely during the lateral movement caused by the thermal expansion of the receiver tube.

To reduce the torsional movement in the MS-Trough collector, two lateral torsion boxes in combination with the composite mirrors are used to strengthen the collector module structure to increase rigidity. The outer mirror edges are directly fixed which leads to avoidance of the bending moment due to wind and dead weight forces. This bending moment can result in strong deformation at the outer edges of the mirrors and results in faulty concentration. In commercial PTCs, thick glass mirrors are used that have a maximum hemispherical mirror reflectivity of 94.6 %. According to measurements by NREL, CIEMAT and DLR, thin class mirrors have a hemispherical reflectivity of 96.4 % [32] and are used in the MS-Trough collector to increase the optical efficiency.

In the case of strong wind, the MS-Trough collector is positioned horizontally that allows a significant wind load reduction compared to conventional collector with the same aperture area. The safety-position is presented in Fig. 2 in comparison with the state-of-art collector position. Due to the reduced wind load, the steel structure, foundations and pylons have light-weight and cost saving design allowing reduction of concrete and steel materials.

2.2. Mechanical qualification method

The PTC modules are 12 m long, rotatable and supported by bearings on their outer sides. Due to this, they sag in the center of the module causing deflection that affects the collector optical performance.

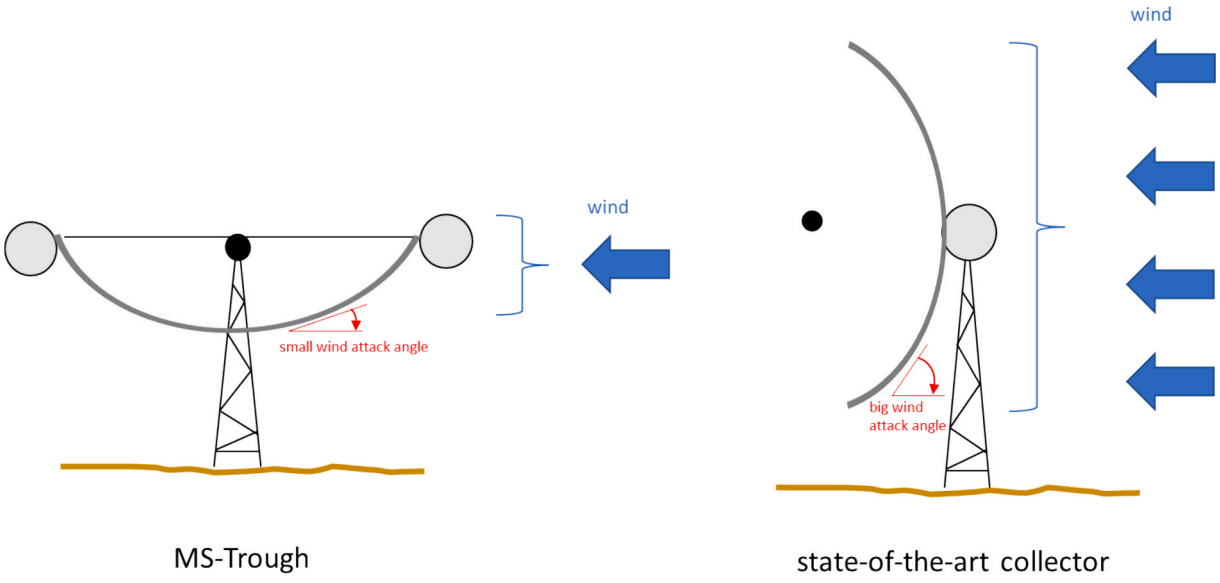


Fig. 2. The "Safety-position" of the MS-Trough collector to reduce wind load.

Rigidity is the most important mechanical property of the PTC which protects the collector against the deflection and deformation of the collector module structure. The mirrors are attached to the collector module structure and the rigidity avoids the deformation of the mirror alignment as well. This leads to more accurate focus of the collector compared to the structures with low rigidity.

2.2.1. Collector maximum deflection measurement

The maximum deflection of the MS-Trough collector in the z-direction occurs as two types of bending first seen by the front beams and secondly by the module itself. The front beams bend because they carry the weights of the torque boxes and mirrors on its outer sides. Additionally, the module itself sag due to its own weight causing the bending.

The maximum bending in the z-direction is reached in the horizontal position (zenith position = 0° position). In this position, the weight forces have the largest lever arm of 3.6 m to the central support point in which the bearing is located. The maximum bending occurs in the z-direction because the moment of inertia of the entire module is smallest in the z-direction. To eliminate the bending stress in the z-direction, the collector should be rotated 90° to the vertical position in which the weight forces acting in the z-direction do not exist anymore as presented in Fig. 3. Therefore, the bending in the both positions (zenith and vertical position) can be compared by aligning a laser over two laser reference points and measuring the distance dL between the measurement reference point and the laser beam as shown in Figs. 4 and 5. The difference between two dL measurements of the zenith and vertical position corresponds exactly to the maximum bending seen by the front beam.

The laser is installed under the mirror at the end of the modules and at the center of the parabolic mirror profile (y = 0). The laser is aligned so that the laser beam passes through both laser adjustment points. For every module measurement, the laser adjustment points 1 and 2 are positioned at the same distance (in the z-direction) from the mirrors. Tis distance is set to be 25.5 mm for module 1, 25 mm for module 2, 23.5 mm for module 3, and 25.5 mm for module 4. Since, the analysis of the bending is based on relative distance measurements, the differences in these absolute values do not affect the analysis results.

Only two inclinations angles (0° and 73°) can be used to measure the maximum deflection due to linearity of the deflection to the line load $\overrightarrow{F_G}$ composed of the gravitational forces acting across the entire surface of the concentrator shown in Fig. 3. The line load has also the maximum component in the z-direction at the zenith position and no component in the z-direction in the vertical position. Based on geometric relationships, the angular dependence of the line load $\overrightarrow{F_G}$ in the z-direction is given by:

$$\overrightarrow{F_G}(z) = \cos\alpha \bullet F_G \tag{1}$$

where α = 0 in the zenith position and α = 90° in the vertical position.

In the vertical position, the deflection is f = 0, as no force is acting; in the zenith position, the deflection is f = maximum, as the entire force acts in the z-direction.

The MS-Trough collector cannot be mechanically rotated to the 90° position but only to the 73°-position. Due to this, 29.2 % of the bending stress remain in the z-direction after rotating the collector to the second position. For α = 73°, cos(α) = 0.292→29.2 %.

The maximum deflection of a beam under a line load $\overrightarrow{F_G}$ and with fixed supports at both ends is presented as follows [33]:

$$f = \frac{\overrightarrow{F_G} \bullet l^4}{384 \bullet E \bullet I} \tag{2}$$

where E is the modulus of elasticity, I is the area moment of inertia and l is the modulus length. E and I are constant as the materials used and their geometric arrangement are the same over the entire module length. The module length l is also a constant value. The only variable is therefore the varying line load, as a result of which the deflection f is proportional to the line load $\overrightarrow{F_G}$. Due to this linear dependence between force stress and deflection, the dependence applies not only to the bending forces but also to the deflection. Therefore, the difference in the distance dL between the zenith and 73°-position presents only 70.8 % of the maximum deflection and the missing 29.2 % is added to the final measurement.

2.2.2. Collector torsion measurement

The collector torsion measurements are conducted without and with the torsion compensators. In both cases, inclinometers of the type SPI-TRONIC PRO 3600 (measuring accuracy ± 0.05°) are used to measure the torsional deformation at the collector ends. The inclinometers are installed at both collector ends on the outer front beams and to the collector center on the front beam of the drive. The inclinometer at the collector center is used to approach various collector positions from both rotation directions of the collector: “south →north” and “north →south”. At the same time, the inclinometers on the outer front beams are used to measure the inclination angles at the collector ends.

The absolute measurement of the inclinometers at the collector ends indicate the torsional deformation but also the imprecise front beam position as the front supports are not aligned exactly horizontally during

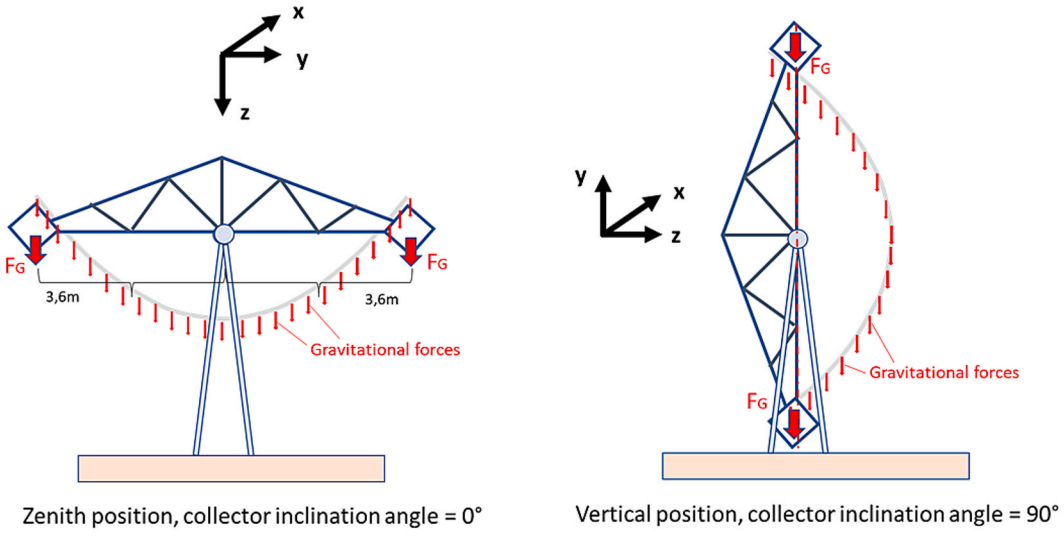


Fig. 3. Load cases of the front beam in zenith and vertical position.

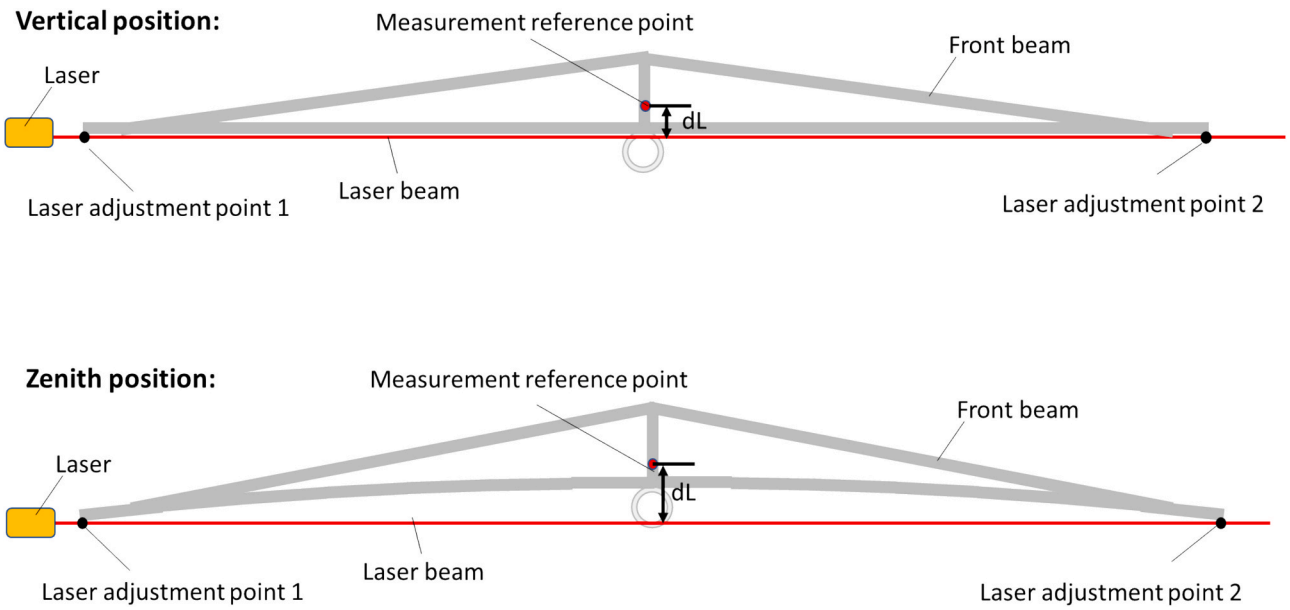


Fig. 4. Schematic representation of the bending measurement of the front beam with a laser.

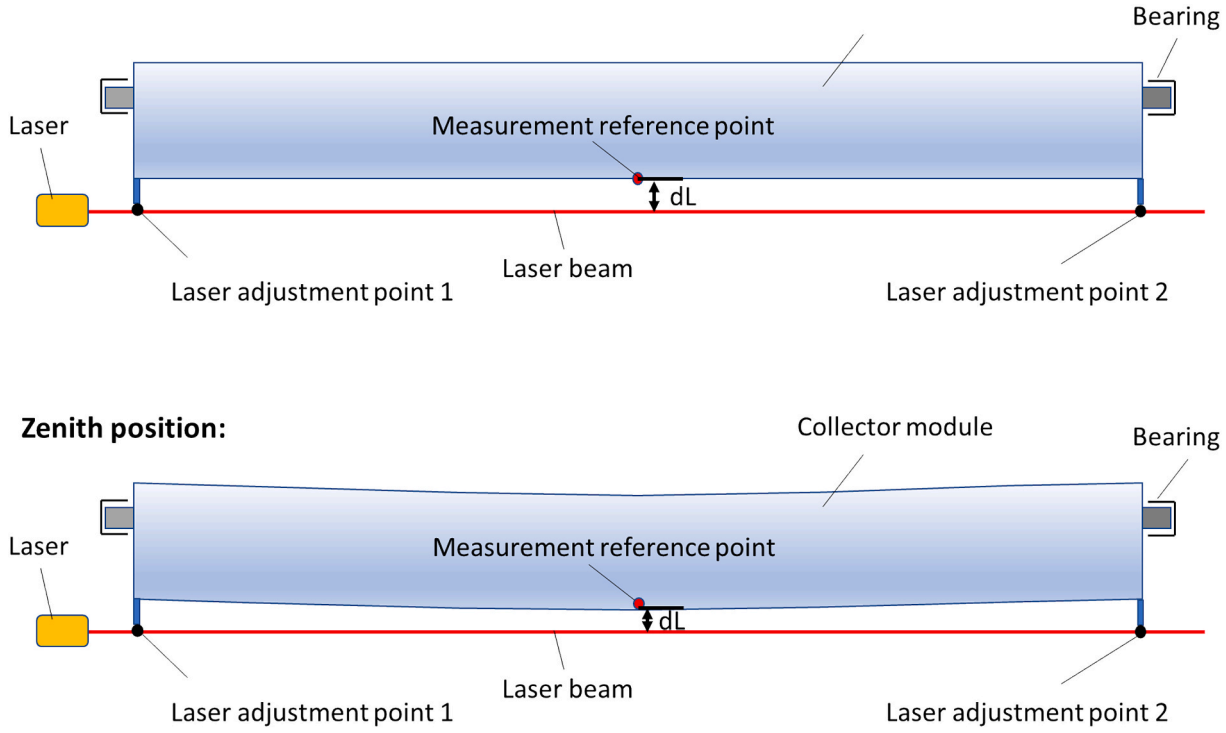


Fig. 5. Schematic representation of the bending measurement of the collector module with a laser.

the module assembly. This measurement is a mixture of two impacts and does not allow a direct evaluation. Due to this, the torsion measurements are performed by using a relative measurement method including the following steps of the procedure:

Giving a target value for the inclinometer installed at the collector center to approach a specific collector position.
Approaching the target value from the rotation direction “south”.
Reading the absolute measured inclination at both collector ends.
Turning the collector 2° further from “south” to “north”.
Approaching the target value again but from the rotation direction “north” instead of “south”.
Reading again the absolute measured inclination at both collector ends.

By following this procedure, the target value is approached from both rotation directions and reached in the same position at the collector center. At the same time, the torsion force affects over the collector and the different values are displayed on the inclinometers at the collector ends than at the center depending on the approaching direction. The difference between the values measured in the center and the collector

ends for the different approaching directions corresponds to the double torsional deformation. This is because the tilt error caused by the imprecise front beam position is eliminated when the measured values are subtracted as follows:

Measured absolute value approached from "south" = tilt error + torsional deformation

Measured absolute value approached from "north" = tilt error – torsional deformation

Measured absolute value approached from "south" − Measured absolute value approached from "north" = 2x torsional deformation

The torsion measurements are conducted with one torsion compensator that is installed at the collector west end. The following weights are used for the torsion compensator: 50 kg, 100 kg and 180 kg. The compensator is used to reduce torsional deformation at the collector ends of the MS-Trough collector. The tests are carried out with different weights to analyze the efficiency of the compensators.

The weight of the compensator generates a permanent torque moment in tracking direction which, at the same time, compensates the bearing friction forces of all bearings between collector center and collector end. By this way, the twisting of the collector is reduced. The same measurement method is used with the compensator than without it. However, the inclinometers are only installed at the western collector end where the compensator is located and at the collector center. Additionally, the collector is moved only to the rotation direction "south-north" because the compensator compensates the bearing friction only in this direction and to other direction the deformation even increases.

The measured absolute values of the torsional deformation without the torsion compensators are used to calculate the absolute ideal values for "0° torsional deformation" but considering the tilt error of the front beam. These ideal values present an ideally rigid collector without torsional deformation but a lightly tilted front beam position. The ideal values are calculated as follows because they exist between the absolute measured values for both rotation directions because the tensional deformation is identical for both rotation directions:

$$\text{Ideal value} = \frac{\textit{Absolutemeasuredvaluefor}''\text{south - north" rotation} + \text{Absolute measured values for "north - south"}}{2}$$

After calculating the ideal values, the above-described torsion measurement procedure is used to measure the inclination at the collector end for different target positions and with different torsion compensator weights. The measurement results are then compared to the ideal values.

2.3. Thermal collector qualification method

The indirect determination of the MS-Trough collector optical efficiency is performed through thermal measurements. To conduct thermal qualification, the collector is focused and cold water is used as heat transfer fluid through the absorber pipe. The test setup includes a cold and a warm water tank, and the Ahlborn Almemo FP-A PT-100 thermocouples (error tolerance ± 0.05 K) at the inlet and outlet of the absorber tube. During the measurements, the outlet hose is held twice in a small plastic tank for 15 s measured by digital stopwatch LAOPAO (error tolerance ± 0.01 s) to define the volumetric flow rate. The collected water is measured by using a calibrated liter meter Rotert-PP-2000 (error tolerance ± 20 ml). The setup is presented in Fig. 6.

While using the measurement setup, the direct radiation DNI is measured by the Kipp & Zonen CHP1 pyrheliometer (standard uncertainty 1.5 %) located close to the collector. The measurements are performed only on cloud- and haze-free days which makes the atmosphere homogeneous.

The optical efficiency (η_{opt}) considers all optical and geometric losses that occur at a vertical angle of incidence ($\varphi = 0$). The ratio between the absorbed heat $\dot{Q}_{abs}$ and irradiated power $\dot{Q}_{DNI}$ defines the optical efficiency with heat losses $\dot{Q}_{loss}$ assuming the vertical irradiation. According to [34], the heat losses for Schott receivers (used in the MS-Trough collector) are 15 W/m at an absorber temperature of 77 K over the ambient temperature.

The ratio is presented in Eq. (3).

$$\eta_{opt} = \frac{\dot{Q}_{abs} + \dot{Q}_{loss}}{\dot{Q}_{DNI}}, \ (\varphi = 0) \tag{3}$$

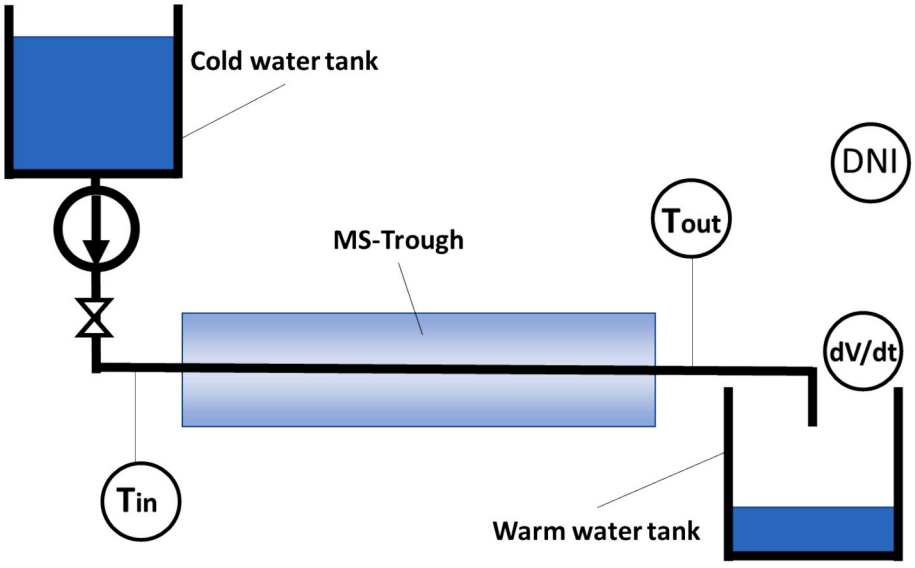


Fig. 6. Measurement setup for thermal collector qualification.

The absorbed heat flow $\dot{Q}_{abs}$ is calculated based on the specific heat capacity c_p, mass flow rate $\dot{m}$ and water temperature change as follows:

$$\dot{Q}_{abs} = \dot{m} \bullet c_p \bullet (T_{out} - T_{in}) \quad (4)$$

The irradiated power is the DNI irradiated onto the aperture surface as follows:

$$\dot{Q}_{DNI} = DNI \bullet A_p \bullet L_K \quad (5)$$

where A_p = aperture width and L_K = mirrored collector length.

2.4. Optical collector qualification method

The optical quality of the collector is measured with the QFly [35] system using Unmanned Aerial Vehicle (UAV)-based high resolution deflectometry measurements. The used UAV is DJI Matrice 210 V2 with the DJI Zenmuse X7 camera. The measurements are conducted for the four Solar Collector Elements (SCEs) of the MS-Trough Solar Collector Array (SCA) for the collector in zenith position.

The rectangular coordinate system presented in Fig. 7 is used when conducting the optical collector qualification. In this system, the Y-coordinate refers to the module length pointing from the front to the rear end of the respective module, the X-coordinate refers to the module width and the Z-coordinate refers to the module height pointing from the parabola apex to the focal line. The key figures of the qualification are the slope deviation (SDx), focus deviation (FDx) and intercept factor (ICsun). The convention is chosen such that positive deviations of the reflector surface (in X-direction) lead to reflections of ideal incident rays above the focal line and negative deviations represent reflected rays below the focal line.

Large-area slope deviation measurements of the modules are conducted by flying the UAV in a special flight path over the collector. The designed flight path, consisting of three sections, is used to capture images from optimized viewing angles for the required analysis steps. In the first section, the flight route is designed such that the best possible camera position accuracy is achieved with photogrammetry. This is followed by a section in which the photogrammetric measurement of the absorber position is performed. Finally, the deflectometric measurement of the reflector shape accuracy is conducted in the last section. The module reflector shape is measured from the images using the absorber tube reflection method in which the distortion of the absorber tube reflection is used as a measure of the reflector shape deviations [35,36].

Within the absorber tube reflection method, the local slope deviations SDx of the reflector surface are determined. These measurements provide quantitative results on the slope deviations of the reflectors from the ideal parabolic shape. Finally, these results are used to derive the spatial distribution of the mirror shape and the alignment accuracy. At the end, the optical collector performance is determined based on a ray tracing analysis.

The intercept factor is derived as a performance indicator from the ray tracing simulations which are based on the measured tilt deviations, modelling the universal sunshape specified in [37] with a half-opening angle of 3.2°, a Circumsolar Ratio (CSR) of 5 %, an angle of incidence of 0° and a nominal absorber tube with a diameter of 70 mm.

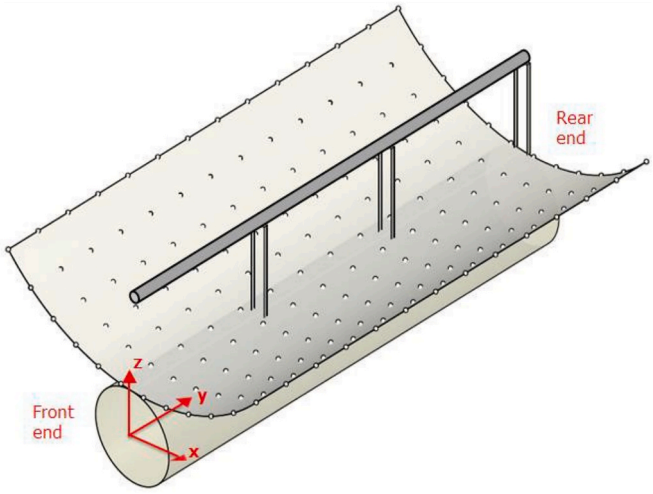


Fig. 7. The rectangular coordinate system of the modules.

3. Manufacturing and construction

3.1. Reflectors

New type of composite mirrors was developed from the conventional composite materials to be installed in the MS-Trough collector. The sandwich design was selected for the panel structure in which a closed-cell polyurethane foam was enclosed in a glass fiber lamination as presented in Fig. 8. Finally, the thin-glass mirror manufactured by AGC Glass Europe Sales SA was glued on the top of the structure resulting in the overall thickness of 30 mm. The mirror modules (unwound width of 4 m and height of 2 m) were manufactured by tfc (tools for composite) subcontracted by Solarlite as a symmetrical half of a parabola with a focal length of 1360 mm and a mirrored aperture width of 6700 mm.

3.2. Structure and drive system

3.2.1. Pile-driven foundation

Conventional PTC collectors require the use of a large volume of concrete in the foundations due to high forces transferred via the foundation. In the case of MS-Trough, the significantly lighter foundation was allowed due to the considerably reduced forces in the new safety-position. The foundation for the MS-Trough was designed to use the pile-driven foundation in which the steel profiles were driving directly into the ground and the unnecessary part of the concrete was removed leading to the high cost and material reduction. To guarantee the stable and precise permanent alignment and positioning of the MS-Trough pylons and the compensation of the foundation forces caused by the collector, a two-foot foundation design was developed and tested. First, two 3 m long double I-100-beams were driven into the ground using a sledgehammer. Next, a concrete casting was placed to the upper foundation section to enable installing of the pylons and to close the connection of the steel profiles to the atmospheric oxygen to avoid corrosion. The A-pylons were used instead of the IPE-400 girders because of causing less shadowing and have a quarter of the steel mass.

A load test was successfully performed with a tensile weight of 1520 kg after setting up the described foundation with pylons on a sandy ground. Based on the distance monitoring system, there was also no detection of the foundation movement due to the load. The forces applied during the load tests reached values that were 1.5 times higher than the forces that would mathematically occur at the wind speed of 90 km/h (max. design value in the solar field). This foundation design can therefore also be demonstrably used with a safety factor of 1.5. The developed and tested foundation design showed a concrete saving potential of > 80 % due to the reduced wind loads and the pile-driven foundation type compared to traditional concrete foundations of PTC collectors.

The design calculations performed by FERRUM show that the MS-Trough standard foundation have a specific concrete consumption of 0.006 m^3/m^2 (related to the mirror aperture area). The EuroTrough pile standard foundations have the following dimensions: diameter of 0.6 – 0.8 m and deepness of 7 – 9 m. [38]. Based on the EuroTrough collector aperture area of 69.12 m^2 (5.76 m aperture width and 12 m module length) [23], the specific concrete consumption for the EuroTrough is 0.029–0.065 m^3/m^2. As the aperture of the MS-Trough collector is 25 %

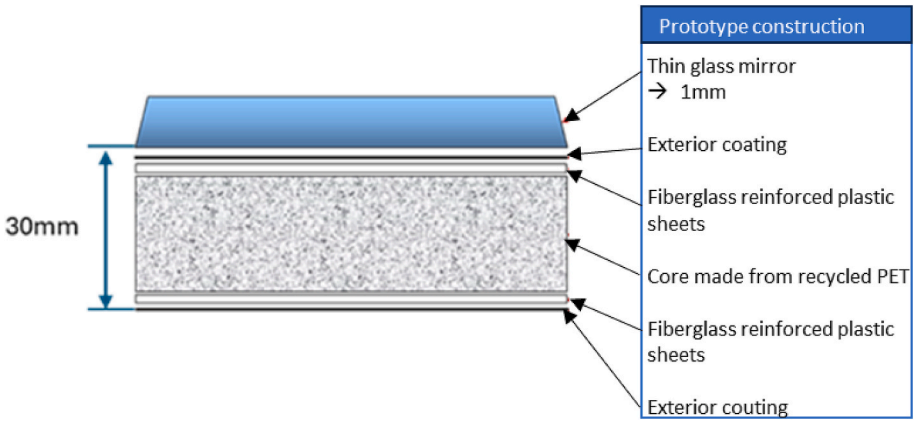


Fig. 8. Sandwich-construction of the mirror prototype.

larger than EuroTrough (7.2 m versus 5.76 m), a direct comparison of the foundations is not straightforward because the foundation load moments do not increase linearly. Although wind forces increase linearly with the aperture area, the distance between the foundation and the point of application of the wind force (the bearing) increases by 25 %, which additionally raises the moment acting on the foundation by 25 %. Taking this factor into account—and assuming a linear relationship between the foundation moment and concrete consumption—the specific concrete consumption for a state-of-the-art collector (with the aperture width of 7.2 m) is calculated to be 0.036–0.082 m^3/m^2. Compared to state-of-the-art collectors, the MS-Trough thus achieves concrete savings of 83.2 % to 92.6 % This result is still preliminary. Further tests are required for final confirmation (e.g., on sandy ground after a prolonged rainy period). The safety factor may need to be increased.

3.2.2. *Torque boxes*

Two separated torsion boxes were developed to limit sagging of the collector module center to a maximum of 5 mm. Within this sagging limit, the optical efficiency of the collector is not sacrificed. The use of thin-walled torsion tubes was first investigated to have low material need and simple manufacturing. However, the results showed a need of reinforcement of the tube structure to maintain the sagging limit of 5 mm which increased the material and installation costs significantly.

The torsion boxes were manufactured as bolted wire mesh boxes to have sufficient stiffness and stability with low material need. The boxes were assembled using pre-galvanized standard angles and a special wire mesh box assembly jig. To ensure the extreme rigidity of the bolted steel structure even under strong wind loads, the most stressed lattice struts were secured against twisting with additional drive-in nails, which were attached using a pneumatic impact bolt.

3.2.3. *Torsion compensators and drive unit*

To avoid a twist of the collector ends due to bearing friction, the patented torsion compensator (Patent reference: DE 10 2015 208 001 B4) in Fig. 10a was tested at the west end of the collector. The twist results in missing a part of the sun rays to the absorber tube. The working principle is presented in Fig. 9. These compensators produce a constant torsion moment in opposite direction to the bearing friction moment. This kind of artificial torsion compensation moment is constant and independent on the collector position angle due to the constant weight and constant diameter of the steel cable guide.

Compared to the State-of-Art collectors, a totally new design of the collector drive system in Fig. 10b was developed. In this new system, the electrical gear motor moves a chain fixed on a radial support. This allows the collector to move continuously instead of stopping for 30 s as in the conventional collector with hydraulic drive system.

3.3. *Assembly of the MS-trough prototype*

The full-scale prototype of the fixed-focus parabolic trough collector was successfully assembled for the qualification purpose. First, all required collector parts were manufactured onsite or shipped to the construction site, such as mirrors, torsion boxes and front beams. Next,

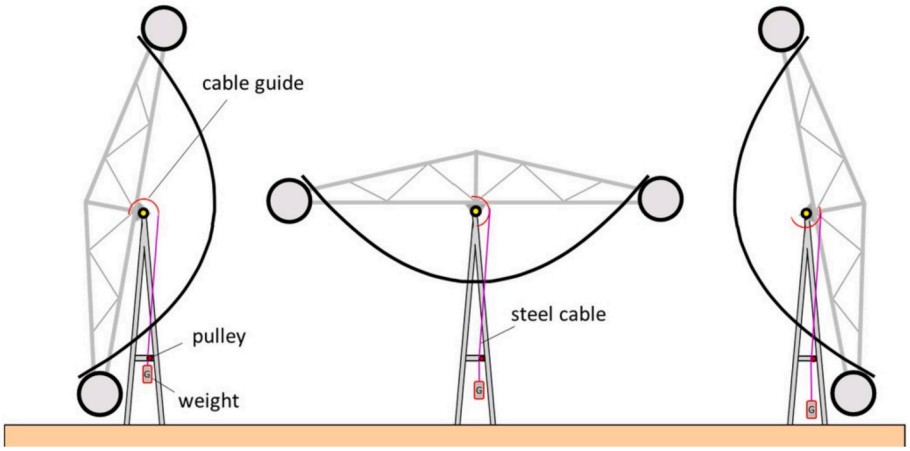


Fig. 9. The MS-Trough torsion compensators working principle.

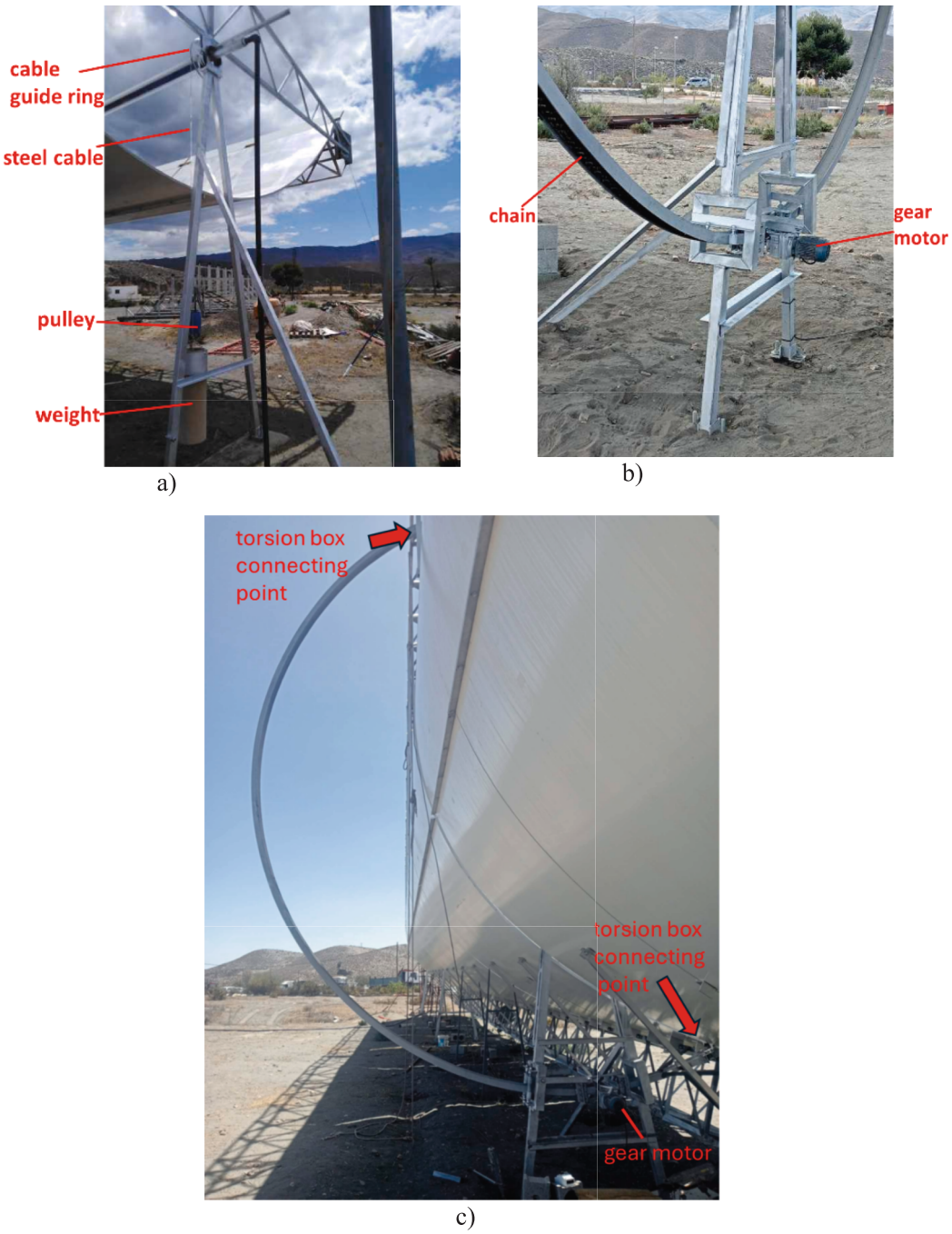


Fig. 10. A) the installed torsion compensator, b) the ms-trough drive system and c) the drive beam of the gear motor.
Source: DLR

the collector mounting JIG and a balancing station for the collector modules were erected. The mounting jig is a support structure which has several plastic mirror support points to ensure a precise mirror position. The mirrors were set on the JIG and the torsion boxes were installed on the sides with the reinforcement supports and the front beams to the module ends as presented in Fig. 11. Four collector modules were assembled using the jig and lifted to the collector pylons which were installed on their pile-driven foundations.

The cavity bearings were installed on the pylons to allow the rotation of the collector modules. The bearings had a slide rail in their interior which allows the absorber tube to slide through the interior during thermal expansion without being rotated by the concentrator. After lifting the collector modules on the pylons, the drive unit and torsion compensator were installed. Finally, the 70 mm standard absorber tubes were installed to the pylons as well. The complete prototype collector presented in Fig. 12 consisted of four 12,3-meter-long collector modules resulting in the overall length of 49,2 m with a mirror aperture of 6.7 m and a total aperture of 7,2 m (considering mirror extension by additional sandwich panel).

During the construction of the collector, it was learned that the use of the precise assembly equipment for the production of all individual components, such as pylon, bearing, torque boxes and front beam, was necessary. The practice also showed that tilting the pylons sideways when handling the modules before hanging them into the bearings helped to avoid mirror breakage and balancing the collector modules was crucial.



Fig. 11. Lifting of the completed collector module from the JIG.
Source: DLR



Fig. 12. The erected MS-Trough prototype collector.
Source: Ferrum

Table 1
Measurements of front beam deformation due to bending stress.

	dL at Zenit (0°)	dL at 73°-position	Difference AB-measurements (70,8 % deflection)	Maximum deflection 100 %
Single front beam West	22.0 mm	20.0 mm	2.0 mm	**2.8 mm**
Double front beam West	25.5 mm	24.0 mm	1.5 mm	**2.1 mm**
Double front beam East	24.0 mm	22.5 mm	1.5 mm	**2.1 mm**
Single front beam East	23.5 mm	21.5 mm	2.0 mm	**2.8 mm**
			Mean value:	**2.5 mm**

4. Qualification

4.1. Mechanical collector measurements

4.1.1. Measured maximum deflection

The MS-Trough collector has two outer single front beams and three inner double front beams. All beams were measured with the laser in the zenith and 73°-position. Only the double front beam in the middle was excluded due to the drive ring which made the laser measurement impossible. The results are presented in Table 1 for the measurements and maximum deflection based on the correlations. The accuracy of the measurements was +/- 0.5 mm due to the laser point diameter.

As shown in Table 1, the measurements resulted in the average front beam deflection of 2.5 mm. The results showed that the outer single front beams at the west and east collector ends deflect 33 % more than the middle beams. In the middle, the beams were double and stabilize each other and therefore were more resistant for the deformation. The outer single beams bent more easily due to the load.

The front beam deformation is specific only to the MS-Trough design and does not occur in conventional commercial collectors. Due to this, it is seen as a disadvantage of the MS-Trough in comparison with the other collector designs. However, the maximum deflection was at the magnitude of few millimeters and can be minimized if the receiver tube is installed 2 mm deeper. Because the front support bending range was from 0.5 mm (morning/evening) to 2.5 mm (midday), lowering the absorber tube results in an optical maximum. After lowering the tube, the distance error to the center of the tube was only 0.5 mm at midday, 0.5 mm in the morning and afternoon and only up to 1.5 higher in the morning and evening. These deviations do not create significant losses.

The results of the maximum deflection caused by the module itself are presented for each module in Table 2. Due to the limitation of the module rotation, the same correction was made for the measurement of the module bending as for the front beam bending.

Table 2 shows the average module deflection caused by the dead weight of 4 mm in the center of the module. The inner modules bent less than the outer modules because their torsion boxes were firmly connected to both adjacent modules. The outer modules were firmly connected only on one side. This resulted in loss of the bending stiffness. However, this property is not specific to the MS-Trough design but occurs also with conventional commercial collectors.

The average deflection of the MS-Trough design is a positive result compared to the commercial collectors. The following two properties of the MS-Trough design enabled to decrease the deflection compared to the state of the art:

- The concentrator has lightweight construction, light composite mirrors and no absorber tube load. These features lower the weight of the concentrator that generates lower bending forces.
- In a combination with the torsion boxes, the composite mirrors are integrated into the collector structure so that they strengthen the bending stiffness of the entire module. This is not a case in the currently available commercial collectors.

4.1.2. Measured torsional deformation

The previously presented relative measurement method (Section 2.2.2) was used to measure the torsional deformation of the MS-Trough collector.

The torsional deformation measurements were conducted on windless days and 13 target positions were approached every 10° from both rotation directions. The measurements were performed first without the torsion compensators for the western and eastern collector ends. The

Table 2
Measurement of module deformation due to bending stress.

	dL at Zenit (0°)	dL at 73°-position	Difference AB-measurements (70,8 % deflection)	**Maximum deflection** 100 %
Module 1	20.5 mm	24.0 mm	3.5 mm	**4.9 mm**
Module 2	22.5 mm	25.0 mm	2.5 mm	**3.5 mm**
Module 3	20.0 mm	22.5 mm	2.5 mm	**3.5 mm**
Module 4	21.5 mm	24.5 mm	3.0 mm	**4.2 mm**
			Mean value:	**4.0 mm**

results showed that the MS-Trough collector exhibits similar torsion deformation for all measured collector tilt angles which indicates a precise collector module balancing. An average torsional deformation of 0.055° was determined at the west end and 0.051° at the east end. The average is calculated by considering the results of all 13 target positions. The higher torsional deformation at the west end can be caused by the fact that the outer west module has neither additional supports between the mirror and torsion boxes, nor does it have lateral mirror bonding with neighboring mirrors. These exist in the outer east module.

The drawback of the torsional deformation measurement of the MS-Trough collector is that it cannot be directly compared with commercial collectors. This is due to the three times shorter length of the prototype collector than the commercial collectors. However, the specific torsional deformation per 12-meter module is comparable. The results show the average torsional deformation of 0.053°, which equals to 0.92 mrad. The corresponding value of the commercial collectors is around 3–12 mrad [27]. The MS-Trough collector has two laterals 12-meter modules, which results in the specific torsional deformation of 0.92 mrad/2 = 0.46 mrad per 12-meter module. The commercial collectors have typically six lateral modules that leads to the specific torsional deformation of 0.5–2 mrad per 12-meter module. In this case, 2 mrad of deformation means an unbalanced collector and 0.5 mrad results in an ideally balanced collector which twists only because of the bearing friction.

The specific torsional deformation of the MS-Trough collector was 8 % lower than the ideally balanced collector. This result is promising because the construction of the MS-Trough collector used around 40 % less steel than typical commercial collector. Additionally, the following reasons resulted in the torsional deformation reduction:

- The lightweight concentrator of the MS-Trough leads to lower bearing load which generates lower bearing friction and thus lower torsion moment as well.
- In the MS-Trough design the mirrors and their support arms contribute to the torsional rigidity.
- The commercial collector modules narrow at their lateral bearings because the 20 cm thick bearing shafts are installed there. The low shaft thickness leads to a significant torsional deformation in this area despite the relatively short shaft length. This critical area does not exist in the MS-Trough design because the torsion boxes are connected end-to-end and narrowing does not occur.
- The receiver tube is fully independent from the MS-Trough collector module and is fixed while the module tracks the sun. The fixed receiver eliminates the need of the flexible pipe connectors of which movement generates additional frictional forces to increase the torsional deformation.

The torsional deformation of the MS-Trough was measured also with three different torsion compensator weights installed to the west collector end. The average torsional deformation resulted in 0.052°, 0.033° and 0.011° with the weights of 50 kg, 100 kg and 180 kg, respectively. The averages are calculated by considering the results of all 13 target positions for each torsion compensator weight. The results show that the deformation was reduced by 79 % when the weight was increase from 50 kg to 180 kg and by 80 % compared to the deformation without the compensator.

4.2. *Indirect determination of collector optical efficiency through thermal measurements*

The experiments for the thermal collector qualification were performed to define the optical efficiency of the MS-Trough collector on the calendar date of 30th of May in 2024. The tests were conducted on the east–west oriented collector at solar noon because the vertical radiation conditions exist at this time of the year and there is no need for IAM-correction. Cold water at the high mass flow rate was used in the experiments to maintain low temperatures (< 50 °C). This enabled to neglect the heat losses in comparison to the absorbed heat energy as explained in the following paragraphs.

To ensure successful optical efficiency test, intensive cleaning of the mirrors and receiver glass was performed, and constant radiation conditions were waited. The results of the experiments with the most favorable test conditions are shown in Fig. 13.

During the test, the direct irradiation (DNI) of 866.7 W/m^2 was measured and the mass flow rate of 2.607 kg/s was determined. In these conditions, the fluid temperature raised from T_{in} = 26.21 °C to T_{out} = 45.17 °C with average temperature of 35.69 °C and the specific heat capacity of 4.179 kJ/kgK was determined at the mean fluid temperature of 35.69 °C. The ambient temperature of 34.7 °C was measured.

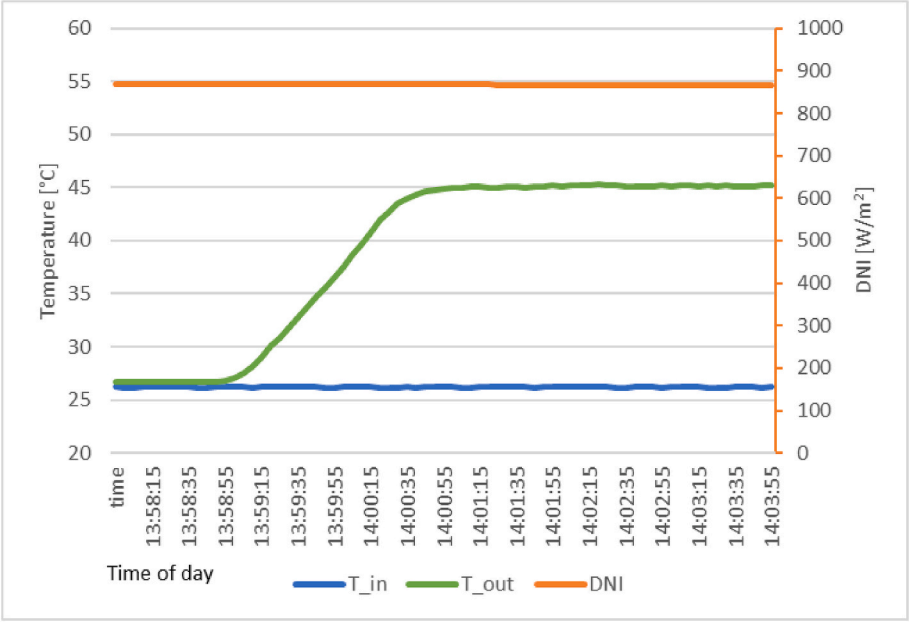


Fig. 13. Inlet and outlet temperature and DNI during the optical efficiency test.

The collector has a mirror aperture width of 6.7 m and the mirrored collector length is 48 m.

Based on the measurements, the absorbed heat flow of $\dot{Q}_{abs} = 206.56$ kW was calculated from Eq. (3). Considering that the absorber temperature is 1 K above ambient temperature and the linear heat loss behavior in the range between 0–77 K [27], the heat losses for 1 K over ambient are **0.2 W/m**. As the receivers are 48 m long, the total heat loss is $\dot{Q}_{loss} = 9.6$ W. When neglecting heat losses from the calculation of the optical efficiency with the measured absorbed heat $\dot{Q}_{abs} = 206.56$ kW, it leads only to an error of 0.005 %. This error is acceptable. The irradiated power from Eq. (4) resulted in $\dot{Q}_{DNI} = 278.73$ kW. Finally, based on Eq. (2) the optical efficiency of 74.11 % was reached, which is within the usual range of optical efficiencies resulted in commercial collectors, such as EuroTrough with 74 % optical efficiency [23]. The MS-Trough collector can reach a higher optical efficiency over 79 % if the mirror quality is increased. The mirrors of the prototype were tested separately in the DLR QUARZ laboratory in Cologne, Germany and the measured intercept factor was only 92 %. Normally, good quality mirror should result in the intercept factor of 98 % in the laboratory measurements. Due to this a very low optical efficiency result was expected for the MS-Trough collector. However, the efficiency was still on the same level than commercial collectors which proofs that the different issues, such as the collector structure in the JIG, the suspension and alignment of the receiver tubes, have not caused any significant additional precision errors. On the contrary, the deflectometric measurements show a higher intercept factor for the collector modules; therefore, the mirror intercept factor must have been improved by pressing the mirrors into the assembly jig. The composite mirror has the intercept factor of 92 % which has high potential to be increased up to 98 %. This would automatically lead to the increased optical efficiency as the intercept factor is included linearly in the determination of the optical efficiency.

4.3. Optical collector measurements

The optical measurements were performed for all four modules of the MS-Trough collector with respect to overall and module specific optical quality indicators: slope deviation (SDx), focus deviation (FDx) and intercept factor (ICsun). In this section, the results of the measurements and ray tracing simulations are presented exemplarily for the first module (SCE1), followed by the results for the whole collector including all four modules.

4.3.1. Determination of the absorber tube position

Normally, the absorber tube position is determined as a part of the QFly measurement procedure to perform the optical collector measurement. In the conventional collectors, the thermal expansion of the absorber tube is compensated by tilting the absorber tube supports. Due to this, an exact determination of the position is required during the measurement. However, the novel, suspended mounting of the absorber tube in the MS-Trough collector compensates the thermal expansion without changing the focal length and the determination of the tube position is not required in the QFly workflow. This allows assuming an almost ideal absorber tube position in the focal line of the collector in the calculation. However, small positional uncertainties caused by the design and manufacturing process were modelled as a shift of ± 5 mm.

4.3.2. Reflector shape accuracy.

Deflectometric measurements were conducted to determine the optical quality of the MS-Trough modules. The results for SDx, mean SDx per mirror panel, and the FDx are presented in the high-resolution diagrams in Figs. 14–16 for the module SCE1, respectively. The color scale of the SDx related diagrams is presented with respect to an ideal parabola and the deviations of the mirror are given in milliradians. The color scale of the focus deviation is given in millimeters.

The mean SDx considers the mean slope deviations of each mirror panel within the range limited by the mirror support points.

The FDx is determined as the deviation of reflected ideal rays from the ideal focal line. The reflected ideal rays are represented by rays coming from the center of the sun, which is modeled as a point source. The diagram of the focus deviation considers the effect of the different distances of the individual mirror elements from the ideal focal line.

4.3.3. Ray tracing analysis of the module performance.

The measured slope deviations were used to conduct ray tracing simulations to define the solar intercept factor ICsun as a measure of the optical performance of the module. An ideal absorber was assumed and the HCE tube was assumed to be in its ideal design position in the focal line. The determined intercept factor value represents the optical performance of the isolated reflector of a stand-alone module and only takes into account deviations of the module structure and mirrors.

The resulting local intercept factors are presented in Fig. 17. Green colored areas represent intercept factors above 95 %, meaning that almost all reflected rays hit the absorber tube. Dark blue areas indicate

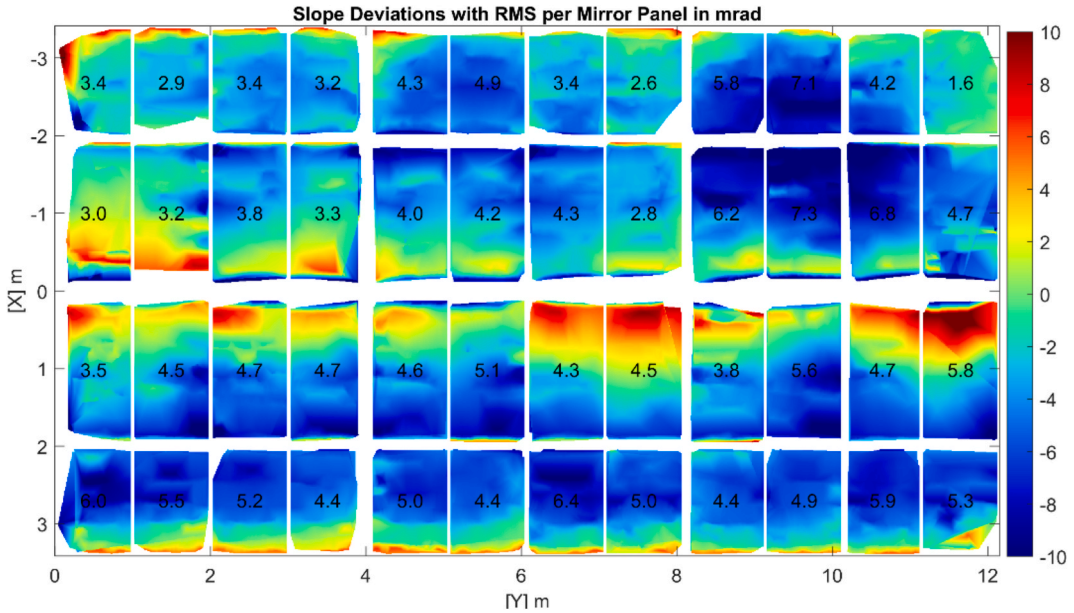


Fig. 14. Slope deviations (SDx) with root mean square (RMS) of each mirror panel for the module SCE1 in milliradians.

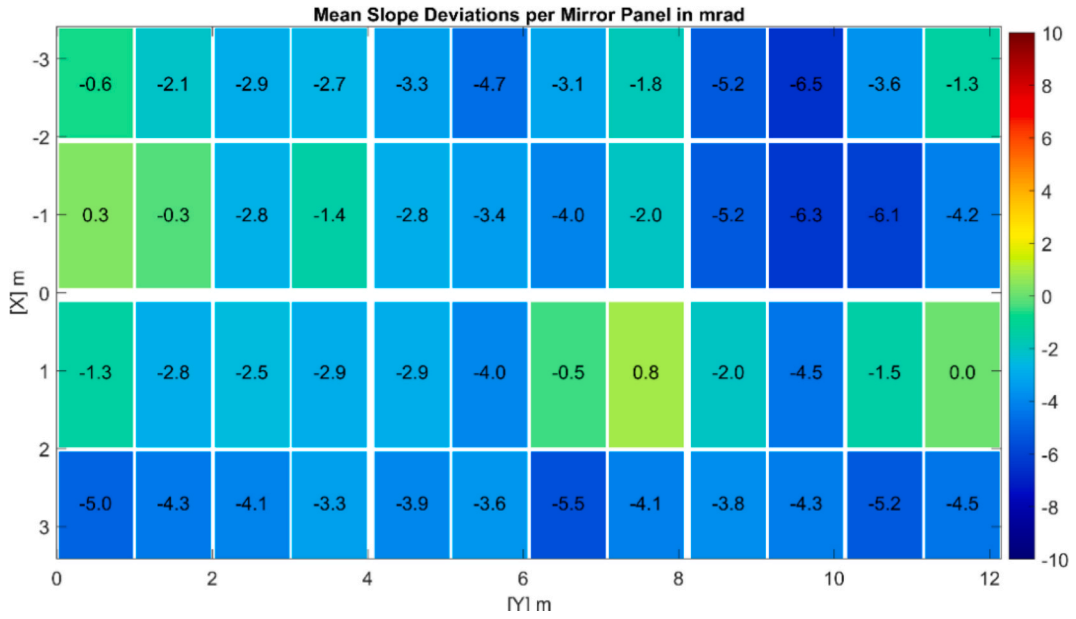


Fig. 15. Mean Slope deviations (SDx) for the module SCE1 in milliradians.

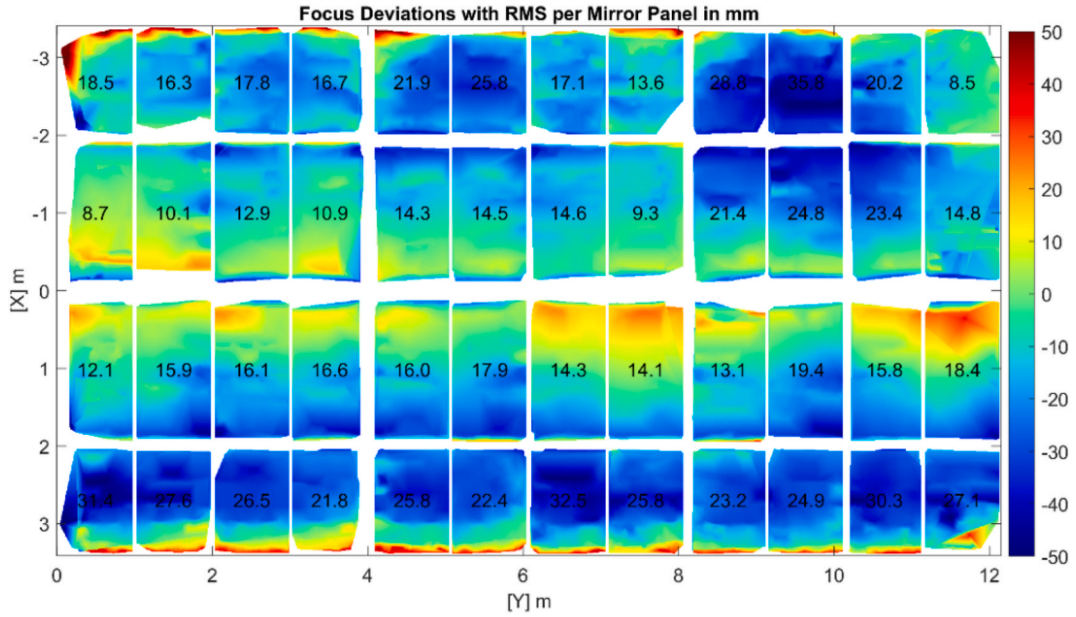


Fig. 16. Focus deviation (FDx) for the module SCE1 in millimeters.

regions of the collector surface for which the rays do not reach the absorber tube.

4.3.4. Performance analysis of MS-Trough collector.

The results for the local SDx of all measured modules SCE1-SCE4 are depicted in Fig. 18a. The results are presented in the collector coordinate system having the East direction on the right side as the modules are mounted from West to East.

In general, it can be seen that the outer rows had more negative root mean square (RMS) SDx values in the range of [-2, −10] mrad while the inner rows had positive values around + 5 mrad. The higher optical quality of the two inner rows was quantified by a lower absolute SDx RMS value. In the case of the modules SCE1, SCE2 and SCE4, the effect of the non-uniform optical quality only had a minor impact on the average intercept factor, which was still above 90 % in all cases.

However, Fig. 18 shows that the optical performance of the SCE3 is clearly worse compared to the other modules. The poorer optical quality of the SCE3 module is not due to manufacturing errors during the mirror production because no irregularities were observed between the mirrors of the different modules during the production phase. The systematically decreasing slope deviation values towards the edge of the collector indicates that the assembly of the mirror surfaces on the SCE3 module caused an unintentional deformation of the mirrors. The inspections after the assembly showed that a screw connection of the mirror clamps was not tension-free and likely caused the deformation in the SCE3. Additionally, during the assembly of module SCE3, the module and crane experienced an unintentional hard touch which may have cause additional deformation of the module.

The results of the slope deviations SDx were used to derive the FDx and ICsun values for the collector presented in Fig. 18(b) and (c),

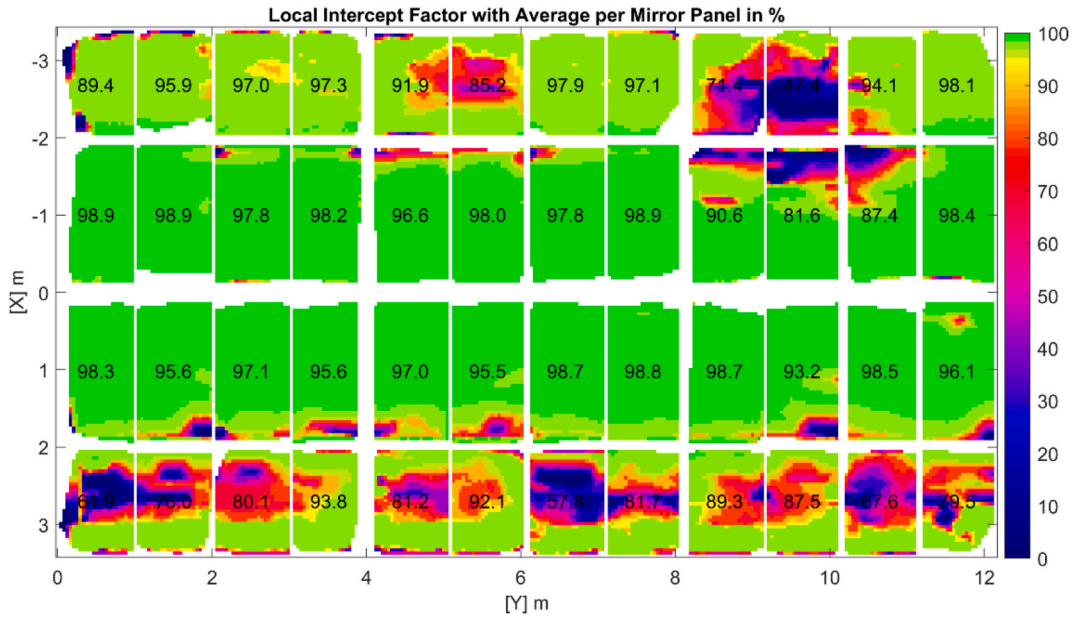


Fig. 17. Local intercept factor (ICsun) for the module (SCE1) in percent.

respectively. The qualitative effects discussed above can be observed in these variables as well.

Based on the entire series of averaged measurements, the quality parameters from the deflectometric shape accuracy analysis of the MS-Trough collector are summarized as follows:

- Slope deviation SDx RMS: (4.97 ± 1.89) mrad
- Focus deviation FDx RMS: (22.8 ± 10.8) mm
- Evaluation area: (82.7 ± 1.6) %
- Average intercept factor: (86.4 ± 15.0) %.

Certain areas of the collector surface are excluded from evaluation during the deflectometry measurement. The excluded areas comprise a 18 mm width border around each mirror facet and the area around the reflection of the receiver supports, leading to an evaluation area value below 100 %. Only the mirror facet border is visible in the above presented diagrams since the support structure reflection location is dependent on the UAV position and is excluded on an image-by-image basis, leaving no visible trace in the global analysis result. The average intercept factor of 86.4 % is below the defined target value of 98 %. However, if excluding the slightly deformed SCE3 module from the analysis, the intercept factor increases significantly to a value of (93.8 ± 3.2) % which is much closer to the target value. The module specific average evaluation results are presented in Table 1.

Based on the measurement results in Table 3, the optical quality varied strongly between the modules primarily driven by the SCE3 module. The fluctuation between the modules is represented by a standard deviation of 1.6 % in the evaluated area, 1.89 mrad in the slope deviation, 10.8 mm in the focus deviation and 15.0 % in the intercept factor. These standard deviations were significantly reduced if only comparing the modules SCE1, SCE2 and SCE4. The reduced set of modules is characterized by a standard deviation of 0.59 mrad in slope deviation and only 3.2 % in the intercept factor.

The systematic difference between the facet rows is presented in Table 4. As shown in Fig. 17 above, the inner mirror rows 2 and 3 performed better compared to the outer rows.

5. Conclusion

In this study, the design, construction and qualification of the novel fixed-focus parabolic trough collector for molten salt applications is presented. The components and MS-Trough collector were manufactured and constructed first time. The following lessons were learned:

- Based on the wind load measurements and mechanical load tests of the light-weight torsion tubes with the wall thickness of 1 mm, the results were satisfactory only if the tubes were reinforced by an additional ribbed structure. Due to this, the torsion boxes were developed and selected as a solution offering the better stiffness with less material usage.
- Due to the strongly reduced wind loads, the MS-Trough design allows to use very small pile-driven foundations to save 80 % of concrete volume. However, the driven foundations with double-T-100 instead of concrete foundations were found to be the correct solution. For aligning the foundations and foundation threaded rods, a template was required and developed.
- The use of the precise assembly equipment for the production of all individual components, such as pylon, bearing, torque box and front beam, was necessary. The practice also showed that tilting the pylons sideways before hanging the modules helped to avoid mirror breakage and balancing the collector modules was crucial.
- Compared to the conventional PTC design, the MS-Trough collector has higher shading losses because of the cavity bearing and new sliding rail to compensate thermal expansion of the receiver tube. This has a negative impact on the Incidence Angle Modifier (IAM) and efficiency.

The qualification of the collector was performed in terms of mechanical, thermal and optical characterization. The results showed that the MS-Trough collector has remarkable low module deflection. The average module deflection was 4 mm which proofs the rigidity of the collector design. The torsional deformation was measured to be 0.055° at the west end and 0.051° at the east end. This resulted in the average of 0.053° (0.92 mrad) and in the specific torsional deformation of 0.46 mrad per 12-meter module which is 8 % less than the EuroTrough collector. The commercially available collectors have the specific torsional deformation of 0.5–2 mrad per 12-meter module. Compared to this, the MS-Trough collector proofs again the high rigidity of the design. Additionally, the torsional deformation was reduced with the patented torsion compensator up to 80 %.

The collector optical efficiency was measured to be 74 %, which is within the usual range of optical efficiencies resulted in commercial

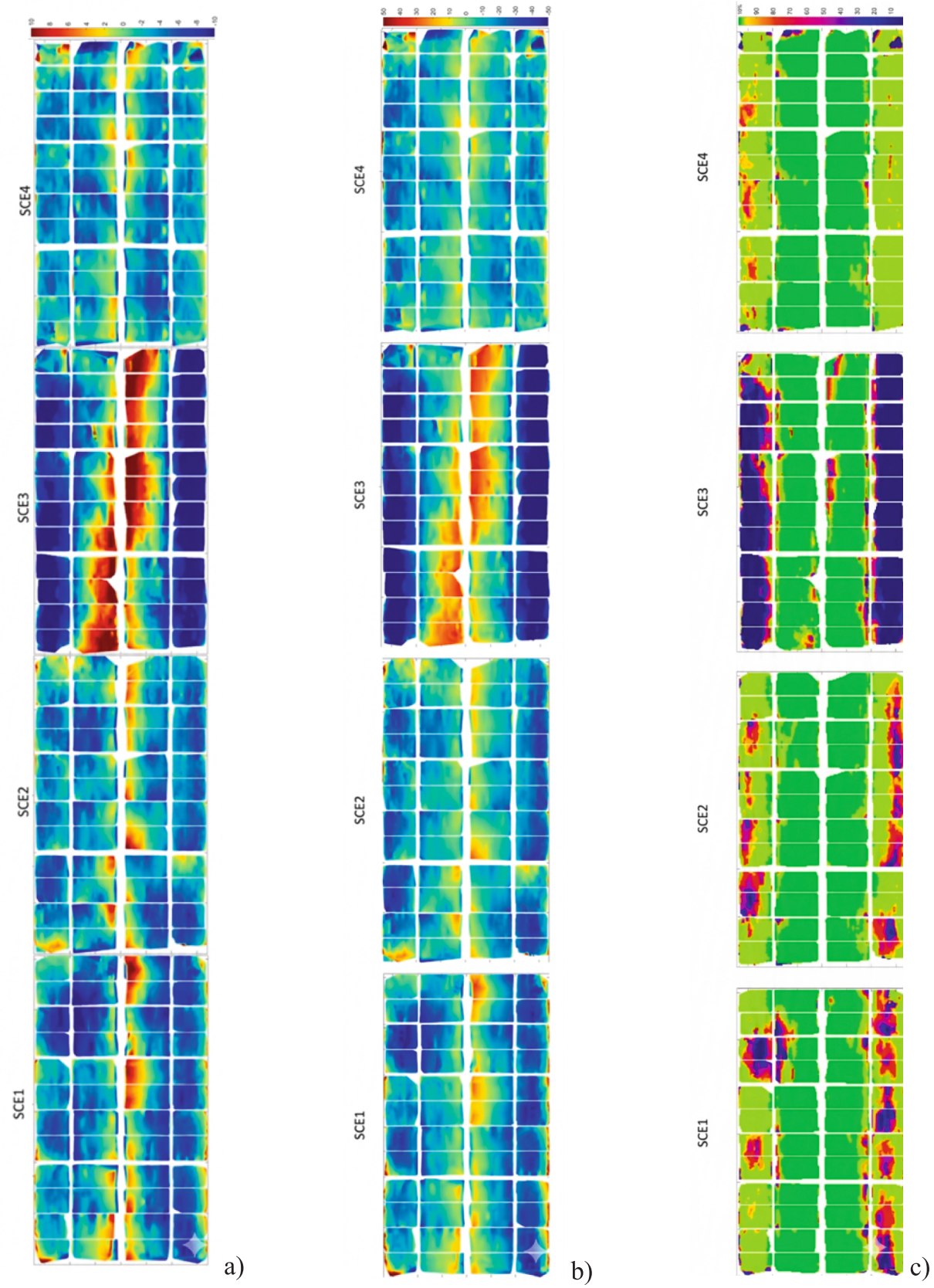


Fig. 18. (a) slope deviations (sdx) for all 4 ms-trough collector modules sce1-sce4 in mrad. (b) focus deviations (fdx) for all 4 ms-trough collector modules sce1-sce4 in mm. (c) intercept factor (icsun) for all 4 ms-trough collector modules sce1-sce4 in %.

Table 3
Summary of the deflectometric measurement results.

Modul	Evaluated area in %	SDx, RMS in mrad	FDx, RMS in mm	ICsun in %
SCE1	85.0	4.71	19.9	90.7
SCE2	82.5	3.93	17.7	93.7
SCE3	81.7	7.71	38.7	64.3
SCE4	81.5	3.55	14.8	97.0
Mean value	82.7	4.97	22.8	86.4
Standard deviation	1.6	1.89	10.8	15.0

Table 4
Summary of the deflectometric measurement results by row.

Row	SDx RMS in mrad	FDx RMS in mm	ICsun in %
Row 1	5.15	28.0	75.6
Row 2	4.32	14.2	97.2
Row 3	4.43	14.6	97.4
Row 4	5.92	31.9	68.2

collectors, such as EuroTrough with 74 % optical efficiency [23]. The efficiency is expected to increase after more careful manufacturing of the composite mirrors. The optical quality of the collector was measured with the QFly method and varied strongly between the modules due to the SCE3 module. The average intercept factor of 86.4 % was measured and was below the defined target value of 98 %. However, if excluding the slightly deformed SCE3 module from the analysis, the intercept factor was increased up to 93.8 %. Additionally, the use of better manufactured composite mirrors and more accurate assembly in the JIG can improve the intercept factor up to 98 %.

The MS-Trough collector was constructed very first time and more experience can improve the qualification results. However, the results already show the competitiveness of the MS-Trough collector design compared to the state-of-art collectors. As future work, the MS-Trough collector demonstration loop is planned to be erected within the EU-funded MSA-Trough project in Évora, Portugal. The loop will be 350-meter long and connected to the balance-of-plant with molten salt as HTF.

CRediT authorship contribution statement

Sonja Kallio: Writing – review & editing, Writing – original draft, Visualization, Validation. **Martin Eickhoff:** Writing – review & editing, Resources, Methodology, Investigation, Funding acquisition, Conceptualization. **Daniel Morales:** Methodology, Investigation, Funding acquisition, Conceptualization. **Timo Zippler:** Methodology, Investigation, Conceptualization. **Kenneth Thiede:** Methodology, Investigation, Conceptualization. **Joachim Krüger:** Methodology, Investigation, Funding acquisition, Conceptualization. **Niels Algner:** Software, Methodology, Investigation, Data curation. **Michael Nieslony:** Writing – review & editing, Software, Methodology, Investigation, Data curation. **Eduardo Saez Martinez:** Software, Methodology, Investigation, Data curation. **Benedikt Kölsch:** Writing – review & editing. **Dirk Krüger:** Resources, Methodology, Conceptualization.

Funding

This work was funded by German Federal Ministry for Economics Affairs and Energy (BMWE) [03EE5082B, 2021–2024] and Centro para el Desarrollo Tecnológico y la Innovación (CDTI) [EXP 00,137,299 / IDI-20210653, 2021–2024].

Declaration of competing interest

The authors declare that they have no known competing financial interests or personal relationships that could have appeared to influence the work reported in this paper.

Acknowledgements

The authors would like to thank the German Federal Ministry for Economics Affairs and Energy (BMWE) and Centro para el Desarrollo Tecnológico y la Innovación (CDTI) for their support and funding of this work. The authors would like to thank also the companies Solarlite Beteiligung UG and Ferrum Tecnoindusrial S.L for their interest and effort to participate to the research project to develop the novel PTC collector.

Data availability

Data will be made available on request.

References

[1] A.H. Alami, A.G. Olabi, A. Mdallal, et al., Concentrating solar power (CSP) technologies: Status and analysis, Int J Thermofluids 18 (2023) 100340.
[2] J. Dersch, M.K. Wittmann, T. Hirsch, Comparison of molten salts and thermal oil in parabolic trough power plants for different sites and different storage capacities, Energies 18 (2025) 1–14.
[3] I.R.E. Agency, Renewable Capacity Highlights. IRENA (2023) 1–3.
[4] E. Carra, Y. Rothenbühler, D. Alarcón, et al., Evaluation of small torsion angles and efficiency in parabolic trough collectors, Energy Convers Manag. 348 (2026), https://doi.org/10.1016/j.enconman.2025.120730.
[5] J. Fredriksson, M. Eickhoff, L. Giese, et al., A comparison and evaluation of innovative parabolic trough collector concepts for large-scale application, Sol. Energy 215 (2021) 266–310, https://doi.org/10.1016/j.solener.2020.12.017.
[6] S.A. Kalogirou, Solar thermal power systems, Sol Energy Eng. (2009) 521–552.
[7] P.V. Gharat, S.S. Bhalekar, V.H. Dalvi, et al., Chronological development of innovations in reflector systems of parabolic trough solar collector (PTC) - a review, Renew. Sustain. Energy Rev. 145 (2021) 111002, https://doi.org/10.1016/j.rser.2021.111002.
[8] G. Saliou, C. Hilgert, R. López-Martin, et al., Segregation of influences on flexible pipe connectors (REPA) force under field operation condition for parabolic trough collector plants, AIP Conf. Proc. (2023), https://doi.org/10.1007/978-3-031-08701-1_2.
[9] I. Biermann, B. Kölsch, S. Kallio, et al., Predictive maintenance of flexible pipe connectors in parabolic trough collectors using artificial neural networks, AIP Conf. Proc. (2026) 1–9.
[10] K. Pottler, S. Ulmer, E. Lüpfert, et al., Ensuring performance by geometric quality control and specifications for parabolic trough solar fields, Energy Procedia 49 (2014) 2170–2179.
[11] A. Maccari, D. Bissi, G. Casubolo, et al., Archimede solar energy molten salt parabolic trough demo plant: a step ahead towards the new frontiers of CSP, Energy Procedia 69 (2015) 1643–1651.
[12] A. Giaconia, G. Iaquaniello, A.A. Metwally, et al., Experimental demonstration and analysis of a CSP plant with molten salt heat transfer fluid in parabolic troughs, Sol. Energy 211 (2020) 622–632.
[13] D. Krüger, S. Penkert, J. Schnell, et al., Development of a concrete parabolic trough collector, AIP Conf. Proc. 2126 (2019) 120008, https://doi.org/10.1063/1.5117626.
[14] L. Martínez-Manuel, J. Córdova-Gallegos, A. Santos, et al., Secondary mirrors for homogenization of parabolic trough radiative flux distributions on cylindrical receivers, Solar Energy 287 (2025) 113209, https://doi.org/10.1016/j.solener.2024.113209.
[15] D. Rodriguez-sanchez, G. Rosengarten, Optical efficiency of parabolic troughs with a secondary flat reflector; effects of non-ideal primary mirrors, Energy 288 (2024) 129521, https://doi.org/10.1016/j.energy.2023.129521.
[16] Y. Abidnoor, F. Lafta, M.A. Al-obaidi, et al., Thermo-hydraulic performance improvement inside parabolic trough receiver tube using passive techniques : a review, Int Commun Heat Mass Transf 169 (2025) 109725, https://doi.org/10.1016/j.icheatmasstransfer.2025.109725.
[17] E. Bellos, I. Daniil, C. Tzivanidis, Multiple cylindrical inserts for parabolic trough solar collector, Appl. Therm. Eng. 143 (2018) 80–89, https://doi.org/10.1016/j.applthermaleng.2018.07.086.
[18] V. Kumar, C. Nonino, S. Savino, On the improvement of the thermal performance of longitudinally finned parabolic trough solar receivers, Appl. Therm. Eng. 279 (2025) 127840, https://doi.org/10.1016/j.applthermaleng.2025.127840.
[19] A.Y. Al-rabeeah, I. Seres, I. Farkas, Experimental investigation of improved parabolic trough solar collector thermal efficiency using novel receiver geometry design, Int J Thermofluids 18 (2027) 100344, https://doi.org/10.1016/j.ijft.2023.100344.
[20] J. Gong, et al., Optimization of a large-aperture parabolic trough solar system with threestage variable-diameter absorber tubes for enhanced efficiency and high outlet temperature, Results Eng. 29 (2026) 108551, https://doi.org/10.1016/j.rineng.2025.108551.

[21] C. Hilgert, C. Jung, K. Schickedanz, et al., Operation of HELISOL®5A in a parabolic trough test loop, Sol. Energy 290 (2025), https://doi.org/10.1016/j.solener.2025.113301.
[22] Maccari A, Donnola S, Matino F, et al. Archimede solar energy molten salt parabolic trough demo plant: Improvements and second year of operation. AIP Conf Proc; 1734. Epub ahead of print 2016. Doi: 10.1063/1.4949195.
[23] E. Lüpfert, E. Zarza-Moya, M. Geyer, et al., EUROTROUGH collector qualification complete performance test results from PSA, ISES Solar World Congress (2003), 2001 & 2003 Proceedings.
[24] M. Geyer, E. Lüpfert, R. Osuna, EUROTROUGH - Parabolic Trough Collector developed for cost Efficient Solar Power Generation. In: 11th SolarPACES International Symposium on Concentrated Solar Power and Chemical Energy Technologies, 2002.
[25] N. Janotte, E. Lüpfert, K. Pottler, et al., Full parabolic trough qualification from prototype to demonstration loop, AIP Conf. Proc. 1850 (2017), https://doi.org/10.1063/1.4984334.
[26] R. Pitz-Paal, J. Dersch, B. Milow, et al., Development steps for parabolic trough solar power technologies with maximum impact on cost, Solar Energy Eng. 129 (2007) 371–377, https://doi.org/10.1115/1.2769697.
[27] G. Hoste, N. Schuknecht, Thermal efficiency analysis of SkyFuel's advanced, large-aperture, parabolic trough collector, Energy Procedia 69 (2015) 96–105, https://doi.org/10.1016/j.egypro.2015.03.012.
[28] A. Mason, E. Reitze, Establishing bankability for high performance, cost reducing SkyTrough parabolic trough solar collector, Energy Procedia 49 (2014) 155–162, https://doi.org/10.1016/j.egypro.2014.03.017.
[29] B. Bierman, C. Treynor, J.O. Donnell, et al., Performance of an enclosed trough EOR system in South Oman, Energy Procedia 49 (2014) 1269–1278, https://doi.org/10.1016/j.egypro.2014.03.136.
[30] S. Bermadinger, M. Steinmair, F. Tiefenbacher, HELIOtube: an industrially realized reinvention of a CSP collector, AIP Conf. Proc. 2126 (2019) 120003, https://doi.org/10.1063/1.5117621.
[31] P. Fairley, In the face of cheap photovoltaics, a Turkish start-up is relaunching solar thermal power, IEEE Spectrum, Access 10.05.2026 (2012). https://spectrum.ieee.org/profile-hittite-solar-energy.
[32] S. Meyen, E. Lüpfert, A. Fernández-García, et al., Standardization of solar mirror reflectance measurements - round robin test. In: 16th SolarPACES Conf, 2010.
[33] MechaniCalc. Beam Deflection Tables, https://mechanicalc.com/reference/beam-deflection-tables (accessed 24 July 2026).
[34] F. Burkholder, C. Kutscher, Heat loss Testing of Schott's 2008 PTR70, Parabolic Trough Receiver. (2009).
[35] C. Prahl, B. Stanicki, C. Hilgert, et al., Airborne shape measurement of parabolic trough collector fields, Sol. Energy 91 (2013) 68–78, https://doi.org/10.1016/j.solener.2013.01.012.
[36] C. Prahl, L. Porcel, M. Röger, et al., Airborne characterization of the Andasol 3 solar field, AIP Conf. Proc. 2033 (2018) 030013, https://doi.org/10.1063/1.5067029.
[37] C.J. Winter, R.L. Sizmann, L.L. Vant-Hull, Solar power plants: fundamentals, technology, systems, economics, Berlin, 1st ed.,, 1991.
[38] P. Dallyn, A. El-Hamalawi, A. Palmeri, Cost-effective parabolic trough foundations for concentrated solar power plants, Loughborough University (2012) 227–238.